Proceedings of the 9th International Conference on Aluminium Alloys (2004)
Edited by J.F. Nie, A.J. Morton and B.C. Muddle

Research and Development of Al-Zn-Mg-Cu-Li Alloys

F. Wei, Z.K. Zhao, P.Y. Liu, T.T. Zhou,

School of Materials Science and Engineering,
Beijing University of Aeronautics and Astronautics, Beijing China, 100083

Keywords: Al-Zn-Mg-Cu-Li alloy, precipitation kinetics; TTT curve; double-ageing,

Abstract

Microstructure control is always of great importance in enhancing properties of high strength aluminum alloys. Attempts to improve the microstructures of 7000 series alloys by the addition of adopting 1%wt lithium have been made in a series of studies. The precipitation kinetics of Al-Zn-Mg-Cu alloys containing 1 wt.% lithium was investigated in comparison with Li free Al-Zn-Mg-Cu alloys both by thermodynamic calculation and by various experimental means, and the aging hardening behavior and relevant microstructural features of the alloys have been evaluated in this paper. The results show that a lithium content at about the 1 wt % level would not make changes in precipitation sequence, but in the precipitation kinetics. It is confirmed from the calculated TTT curves and microstructural investigations that lithium in general retards the precipitation process although it promotes nucleation of precipitates in the initial stage. The resulting aging behavior and aging hardening curves are therefore unusual. Duplex aging processes must be taken into account for obtaining maximum hardness as opposed to aging at 120℃ as ordinarily done for Al-Zn-Mg-Cu alloys.

1. Introduction

Al-Zn-Mg-Cu alloys are playing a very important role in aerospace and automotive industries due to their high specific strength and other valuable properties. Alloying adjustment and microstructure control have always been taken as efficacious measures in gaining further improvement of the alloys' performance. Therefore there has been a great deal of work in this aspect over a long period of the time. The function and effects of lithium in aluminum alloys are well understood and 8000 series of Aluminum-lithium alloys have been developed and applied in the important fields as aerospace industry because of their attractive characteristics of light weight, high specific strength and high elastic modulus. It is well known that the main strengthening precipitates are δ or its transient phases in the alloys with relatively high content of lithium above 1.8%wt [1-3]. On the other hand the maximum strength of Al-Zn-Mg-Cu alloys is generally associated with precipitates of η' phase and its precursors.

The pronounced hardening response to peak ageing for 7075 alloy at 120℃. There has been little systematic investigation on the phase transformation or precipitation kinetics, microstructure evolution and hardening effect of Al-Zn-Mg-Cu alloys with lithium about

1.0%wt or below, although it has been reported that the δ phase is not found in these alloys [2,4,5]. The purpose of the present work is to put raise interest in Al-Zn-Mg-Cu-1%Li alloys and to provide a deep understanding of the effects of lithium in the alloys in the search for possible Li containing high strength alloys with good performance.

2. Experimental Details

2.1. Experimental Materials

The materials investigated are Al-Zn-Mg-Cu alloys containing lithium about 1.0wt%. The nominal compositions of which are shown in table 1.The alloys were melted in a vacuum furnace and cast into a water-cooled mould under argon protection. The ingots were homogenized through two step-heating, 430℃ for 24h and 470℃ for 36h, then hot forged at about 430℃ .

Table 1: Compositions of tested materials *wt*%.

Alloy	Zn	Mg	Cu	Li	Zr	Mn	Cr	Er	Al
A	5.14	1.24	1.76	-	0.1	0.35	-	-	Bal
B	5.17	1.22	1.74	1.01	0.1	0.35	-	-	Bal
C	5.6	2.8	1.6	-	-	-	0.24	-	Bal
D	5.6	2.8	1.6	1.1	-	-	0.24	-	Bal
E	8.0	2.4	2.4	-	0.18	-	-	-	Bal
F	8.0	2.4	2.4	1.1	0.18	-	-	-	Bal
G	5.6	1.9	1.6	-	-	-	-	0.3	Bal
H	5.6	1.9	1.6	1.0	-	-	-	0.3	Bal

2.2. Experimental Methods

2.2.1. Microstructure Analyses by TEM

Transmission electron microscopy (TEM) was used in microstructure analyses. Slices of 3mm in diameter were cut from alloys and ground to a thickness of about 50μ.The disks were subsequently polished to perforation in a twin-jet electro-polishing unit using a methanol-70% methanol solution held at about -30℃.The thin foils were examined in a TEM-2010 FS microscope.

2.2.2. Precipitation Kinetics Study by DSC

Differential scanning calorimetric (DSC) techniques were adopted to study the kinetics of precipitation and dissolution of GP zones and metastable phase η′ in the alloys. It is generally accepted [10] that the precipitation sequence of 7000 alloys is as follows,

$$\alpha \rightarrow \text{GP} \rightarrow \eta' \rightarrow \eta(MgZn_2)$$

In the process there may be overlap of one transformation with another, and peaks on DSC curves may be overlapped by one another. In order to obtain precise information from the phase transition the calorimetric method was used for determination of exothermic doublet and endothermic doublet in specimens with different initial phases. Specimens with three different pretreatments were used as follows: as solution treated without any precipitate;

low temperature aged , at 70℃ for240h or at 120℃ for 24h, mainly with GP zones; and high temperature or two-step artificial aged at 120℃ for 3.5h and 160℃for 12h with η′ as main precipitate. The endothermic peak on the DSC curves appearing in heating process was assumed to represent dissolution of the initial phases. The tests were made to alloys A and B, using Pheometric Scientific DSC SP， and with heating rate of 10 °C /min.

2.2.3. Precipitation Kinetics Study by SAXS

The precipitation kinetics was investigated also by small angle X-ray scattering (SAXS) method. The samples from alloy A and B underwent mechanical polishing to the shape of thin wafers of approximately 0.07mm in thickness. A conventional X-ray tube with Cu anode was used with Ni filters in order to get a CuK_α source ($\lambda = 1.541\dot{A}$). A light sensitive detector was used to measure the scattering results. Spectra were corrected for background, fluorescence and absorption effects. The particle dimensions were calculated using the Guinier approximation, which gives the gyration radius of particles [6].

$$I \propto \exp(-\frac{h^2 R^2}{3})$$

The Guinier plot (ln(*I*) vs. q^2) shows a strait line in a wide range of scattering vectors, where R is the effective precipitate radius and h is the scattering vector. For spherical particles, the gyration radius is $\sqrt{3/5}$ of the effective radius. For non-spherical particles, the gyration radius was dealt with approximation equal to the radius of a sphere with equal volume. The integrated intensity $Q_0 = \int_0^\infty Iq^2 dq$ was calculated from the X-ray scattering spectra and related to the volume fraction through the following equation:

$$Q_0 = 2\pi^2 f_v (1 - f_v) \frac{(\Delta Z)^2}{\Omega^2}$$

where f_v is the precipitated volume fraction, Ω is the atomic volume and ΔZ is the difference in average atomic number between the precipitates and matrix, which was calculated assuming that the precipitates had the composition of the equilibrium η phase $MgZn_2$.

2.2.4. TTT Curve Determination

Thermal dynamic calculations were adopted in the present work making use of Avrami-Johnson-Mehl (AJM) equation and one heating rate method in helping with the analysis of phase transition and kinetic parameters for GP zones and η′ phase dissolution. TTT curves (commonly used in steels) are difficult to establish in aluminum alloys because the solid solution composition is continuously changing [7]. Hence there are relatively few studies on TTT curves in aluminum alloys in the published literature. In the present paper we gain kinetic formulation by substitute parameters and achieve TTT expression by its physical meaning and mathematical analysis. It is demonstrated that the TTT results are consistent with experimental results of the alloys.

2.2.5. Aging Behavior

The aging behavior and precipitation hardening effects were studied by Vickers hardness testing of aged specimens for alloys C,D,E,F,G,H, with the testing load of 1000g. The specimens were generally solution treated at 490℃ for 1h, and then water quenched. They were artificially aged at various temperatures with different holding time, or treated by two-step ageing at 110℃, followed by further ageing at 160℃.

3. Results and Discussion

3.1. Kinetic Parameters for the Dissolution of GPB Zones and η′ Phase

The specimens (A and B) of Al-Zn-Mg-Cu alloys with or without Lithium used for kinetic parameters analysis were treated with different aging process in order to develop different initial phases in the alloys. There are mainly GPB zones in alloys aged for 240h at 70℃ or 24h at 120℃ and η′ phase after two-step ageing at 120 ℃for 3.5h and 160 ℃for 12h. Kinetic parameters for GPB zone dissolution and for η′ phase dissolution were investigated according to the correspondent endothermic peaks in DSC curves .The dissolved fraction (mole fraction, *Y*) and the dissolution rate (d*Y*/d*t*) calculated by using equation (1) and (2) (which are Avrami—Johnson—Mehl equation generally adopted in describing isothermal phase transformations or the precipitation kinetics), are functions of the aging temperature. *Y*（*T*）,is here defined as the ratio of the area *A*（*T*） enclosed by the peak at temperature (T), to the whole area of peak, A_f

$$Y（T）=A（T）/A_f \quad (1)$$

The transformation rate（*dY/dT*）is related to the heating rate (*Φ*) for the DSC scan by

$$dY/dt=（dY/dT）（dT/dt）=Φ（dY/dT） \quad (2)$$

Kinetic parameters for the dissolution of GPB zones and η′ phase in both kind alloys derived from to the DSC curves and relevant equation are shown in Table.2.

Table.2.Kinetic parameters for dissolution of GP zones andη′phase.

Parameter	GP dissolution (For 240h at 70℃)		GP dissolution (For 24h at 120℃K)		η′ dissolution (Two-step aging)	
Samples	A	B(with Li)	A	B(with Li)	A	B(with Li)
Peak(K)	430±3	431±3	468±3	472±3	478±3	494±3
Q(kJ.mol^{-1})	100±6.4	95±7.4	102±6.6	103±6.9	93±7.5	173±6.2
k_0(min^{-1})	7.18×10^{11}	2.94×10^{9}	7.98×10^{9}	7.0×10^{10}	9.80×10^{7}	3.19×10^{16}

Notes：Two-step aging indicates the process of 3.5h at120℃ and then 12h at 160℃.

The activation energy values of alloy A (without lithium) show good agreements with the values of the phase dissolution in 7075 alloy determined by the varying heating rate method as reported by Delasi *et al.*[8,9], which are 108.0±6.7kJ/mol for GPB zone dissolution and

86.2±7.1 for η′ phase dissolution. Comparing the activation energy values for GPB zone dissolution in 7075 and in alloy A with that in alloy B (containing 1wt%Li), they are the same within experimental error. On the other hand, the activation energy values for η′ phase dissolution in the above two alloys are 93±7.5kJ/mol and 173±6.2kJ/mol respectively，as demonstrated by the results from the two-step aging process .This is a very significant change in activation energy and, hence, we can conclude that Li has little effect on GPB zone dissolution but either postpones the transformation of η′ phase or increases its stability.

3.2. Determination of TTT Curves

The commonly adopted aging temperature for Al-Zn-Mg-Cu serial alloys is between100℃ and 180℃, for the reason that the aging time needed will be too long if the temperature is lower, and the microstructure tends to coarsen readily when the temperature is too high. In this paper, TTT curves are plotted to the temperatures in the above range. The expression (3) was derived to describe the changes of transformation amount at temperature *T* with holding time *t* by modifying equation (1) and substituting equation (2). TTT curves are then derived by considering the characteristic times at 0.05 and 0.95 transformation for beginning and completing of these isothermal transformations from expression (3).

$$T=Q \cdot R^{-1} \cdot [ln k_0 - ln ln (1-Y) + ln t]^{-1} \quad (3)$$

The TTT curves obtained are shown in Figure 1, where the temperature for abscissa , time for ordinate, the values of *Q* and k_0 are in Table.2. Here the kinetic parameters for GPB zones transformation are selected as $k_0=7.98\times10^9$ min^{-1} , Q=102±6.6kJ.mol^{-1} referring to the Al-Zn-Mg-Cu alloy and $k_0=7.0\times10^{10}$ min^{-1}， Q=103±6.9kJ.mol^{-1} referring to the Al-Zn-Mg-Cu-1.0%Li alloy.

The kinetic parameters for η′ phase transformation are selected as $k_0=9.80\times10^7$ min^{-1}， Q=93±7.5kJ.mol^{-1} referring to the Al-Zn-Mg-Cu alloy and $k_0=3.19\times10^{16}$ min^{-1}， Q=173±6.2kJ.mol^{-1} referring to the Al-Zn-Mg-Cu -1.0%Li alloy. In Figure 1. A (E) and B(F) stand for beginning and completing of GPB zones transformation in the Al-Zn-Mg-Cu (Al-Zn-Mg-Cu -Li)alloy ,C(G) and D(H) for beginning and completing of η′ phases transformation in the Al-Zn-Mg-Cu (Al-Zn-Mg-Cu -Li) alloy.

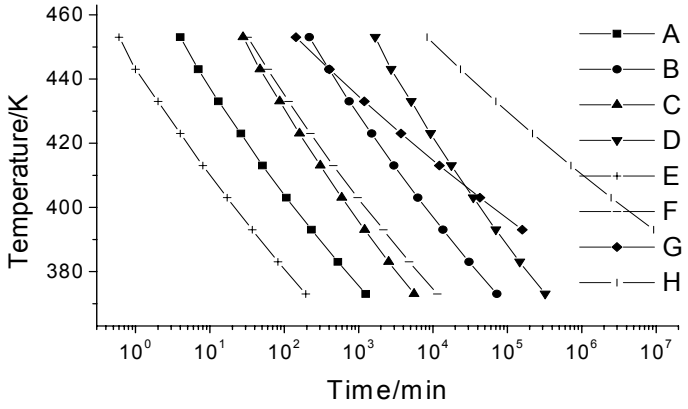

Figure 1: TTT curves for GPB zones and η′phase transformation. A (E) and B(F) stand for beginning and completing of GPB zones transformation in Al-Zn-Mg-Cu (Al-Zn-Mg-Cu -Li)alloy, C(G) and D(H) for beginning and completing of η′phase transformation in Al-Zn-Mg-Cu (Al-Zn-Mg-Cu -Li)alloy.

It can be concluded from the TTT curve that, in general, lithium retards the precipitation process but promotes nucleation of precipitate precursors such as GP zones

3.3. The Microstructures Analyses by SAXS and TEM

Since the precipitates and precipitation sequence in Al-Zn-Mg-Cu alloys at various aging conditions are well confirmed the microstructure investigation in this paper is focused on the lithium containing alloys. The precipitates in the alloy B aged at 120℃×24h or lower temperature and the precipitates in the alloy B aged at 160℃,180℃ or two-step aging(120℃×24h and 160℃×3.5h) have been determined to be GP zone for the former and η′ phase for the latter respectively, Figure 2,3,4. There is no diffraction of superlattice found in the selected area electron diffraction patterns in the former, which is to say that GP zone should be main precipitates in the samples, other than η′ phases. It is well established that η′ phases is dominate phase in samples after higher temperature aging or two-step aging. These results indicate that the precipitates and precipitation sequence in Li-containing alloys is in line with that in Li free alloys.

The morphology, dimension and distribution of the precipitates in the alloys with or without lithium were observed to develop an understanding of their coarsening process. The SAXS method was also used in assisting the study. The results showed that the precipitate size in Li-containing alloys is inevitably smaller than that in Li-free alloys if the alloys undergo the same aging process, and the morphology of the precipitates is changed, with η′ phases taking spherical shape in Li-containing alloys and column in Li-free alloys, see Figure 5.

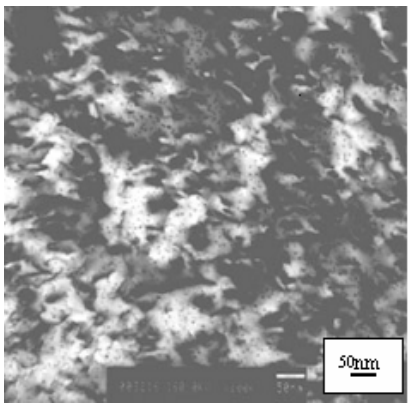

Figure 2: The morphology of bright field of the alloy containing 1.0%Li aged after 120℃×24h.

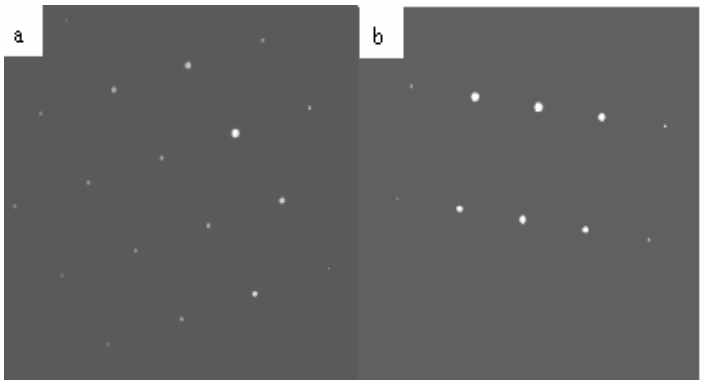

Figure 3: The selected area electron diffraction patterns of alloy containing 1.0%Li aged after 120℃×24h with (a) $B=[110]_{Al,}$ (b) $B=[112]_{Al.}$

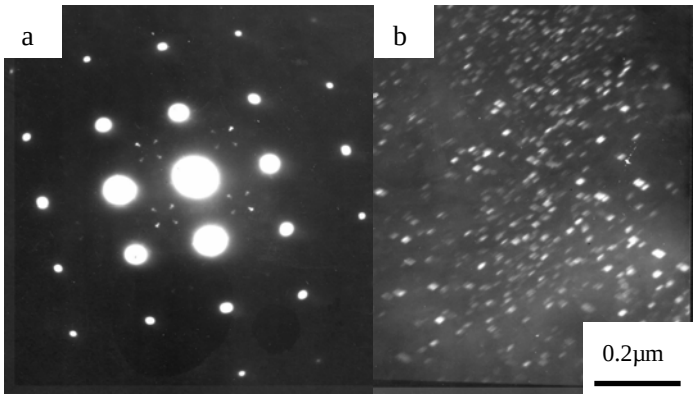

Figure 4: The selected area electron diffraction patterns with super lattice image, SAED (B=$[100]_{Al}$) (a) and the dark field morphology of super lattice spots (b) of alloy containing 1.0%Li after two-step aging.

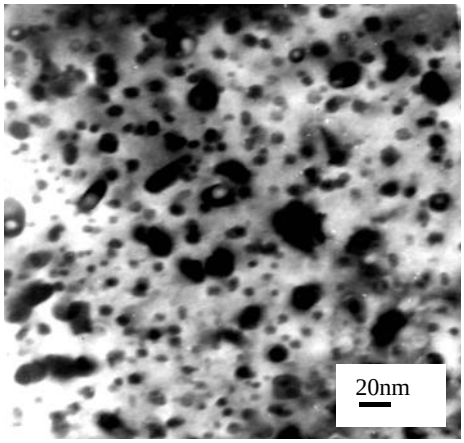

Figure 5: Precipitates in alloys with 1.0%Li ,180℃×32h.

The evolution of precipitate size and volume fraction of alloy B at different aging conditions has been determined by means of SAXS measurements. The results showed that the shapes of the precipitates in Li-containing alloys could be classed as ellipsoids of revolution. The precipitate size is some nanometers. The coarsening behavior of the precipitate has been quantified with LSW model. The maximum precipitate volume fraction is about 0.023- 0.028 and the Maxwell distribution of precipitate mass with gyration radius has been constructed from the SAXS measurement results and is shown in Figure. 6.

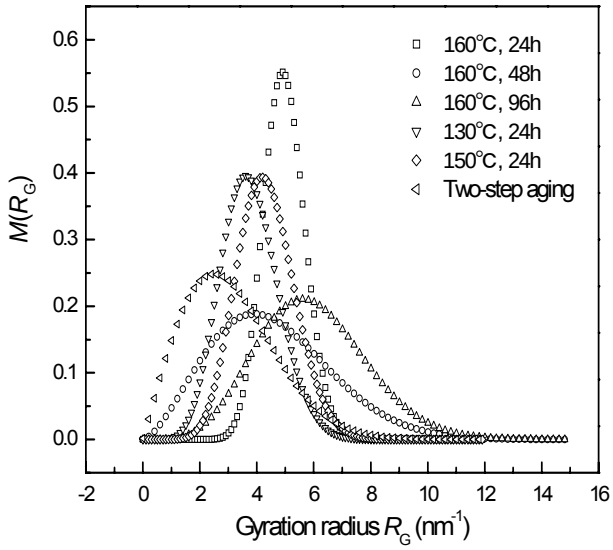

Figure 6 Maxwell distribution diagram of precipitate mass with gyration radius for the alloys aged at various conditions

3.4. Hardening Effects

Vickers hardness testing was carried for aged specimens of alloys C,D,E,F,G,H, and the hardening curves for alloy D are shown in Figure 7.

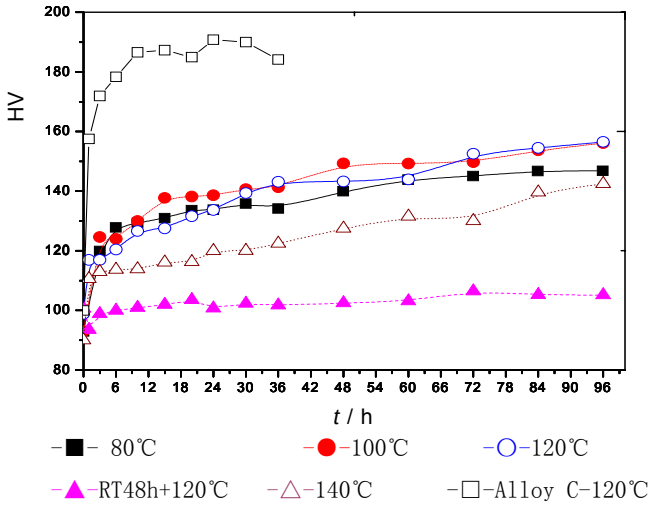

Figure 7: Hardness curves of alloy D(Li-containing)aged at 80℃,100℃,120℃,140℃,or natural ageing for 48h followed by 120℃ ageing in comparison with alloy C(Li free) aged at 120℃.

It can be seen from the aging curves that the aging response of the Li-containing alloys is much weaker than that in the alloys without Li. However, it is well known that the hardening effect can be enhanced remarkably for the Li-containing alloys if pre-aging is taken either at 120℃ or at temperatures below 120℃ then followed by secondary step aging at 140℃ or 160℃. As the result of two-step aging the hardening effect of Li-containing alloys is equivalent to that of Li free alloys, Figure 8.

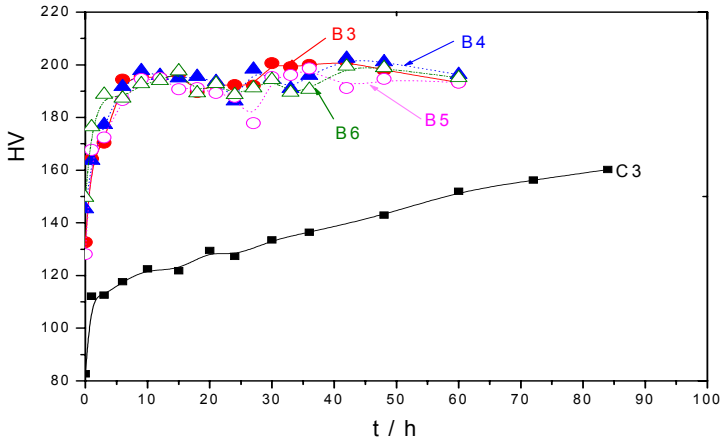

C3-■-120℃, B3-●-80℃×5h+100℃×5h+160℃, B4-▲-80℃×5h+100℃×5h+120℃×5h+160℃
B5-○-RT100h+80℃×5h+100℃×5h+160℃, B6-△- RT100h+80℃×5h+100℃×5h+120℃×5h+160℃

Figure 8: The effect of two-step ageing on the hardening effect of alloy D

The reason for the changes in the precipitation behavior by addition of 1wt% lithium to Al-Zn-Mg-Cu alloys has been discussed and concluded as follows.

There are two types of GP zones reported in Al-Zn-Mg based alloys, which are solute rich GP Ⅰ zones, or Mg/Zn cluster; and solute/vacancy-rich GP Ⅱ zones. GP zones form at low-temperature region and usually keep stable below 140 ℃.When aging to the temperatures above the solidus of GP zones ,GP Ⅱ zones and GP Ⅰ zones larger than a critical size transform to the η′phase, while GP Ⅰ zones below the critical size dissolve in the matrix. [10,11].

Li atoms possess high vacancy-binding energy and preferentially trap the quenched-in vacancies forming Li-VRC clusters. The reduced free vacancy concentration retards the diffusion of Zn and Mg atoms and consequently suppresses the formation and coarsening of GP Ⅱ zones and η′ phases. However the formation of GP Ⅰ zones is accelerated in that Li as solute atom will decrease the solubility of Mg and Zn in matrix promoting their precipitation, but their growth will be suppressed. All of these features have been exhibited by the TTT curves shown in Figure 1. Meanwhile the solidus of GP Ⅰ zones in the Li-containing alloys increases. Then, because there are smaller and fewer GP zones in the alloys with lithium subjected to one-step aging, the maximum hardening effect is not reached. When the two-step aging process is applied to the lithium containing alloys both GP zones formed in pre-aging remain to the temperature at which second step aging is taken and a sufficient η′ phase precipitate population is developed to give rise to higher aging hardness.

4. Conclusions

- Lithium content about 1 wt % in Al-Zn-Mg-Cu alloys does not alter the precipitation sequence, but does affect the precipitation kinetics.
- It is confirmed from the calculated TTT curves and microstructure investigations that lithium in general retards precipitation process but promotes nucleation of precipitates in the initial stage.

- In the lithium containing alloys the maximum hardening effect can not be obtained by aging at single temperature but by duplex aging process, firstly at temperature of 120℃×24h(or plus lower temperature stage) and secondly at 140℃-160℃

Acknowledgement

The authors would like to acknowledge the financial support from Foundations of National Basic Research Priorities Program (973-G19990649) and High-Tech Research & Development Program (863).

References

[1] Dinsdale K, Noble B, Harris S J. Development of Mechanical Properties in Al-Li-Zn-Mg-Cu alloys. Materials Science and Engineering. A104(1988), p75—84.
[2] A.Sodergren and D.J.Lloyd. The influence of lithium on the aging of a 7000 series alloys. Acta metall., 36(8)(1988), p2107—2114.
[3] P.J.Gregson, K.Dinsdale, S.J.Harris and B.Noble. Evolution of microstructure in Al-Li-Zn-Mg-Cu alloys. Materials Science and Technology, 3(1987), p7—13.
[4] Z.W.Huang , M.H.Loretto，R. E. Smallman and J.White. The mechanism of nucleation and precipitation in 7075-0.7 Li alloys. Acta.Metall.mater, 42(2)(1994) ,p549--559 .
[5] Z.W.Huang, M.H.Loretto and J.White. Influence of lithium additions on precipitation and age hardening of 7075 alloy. Materials Science and Technology, 9(1993), p967—980.
[6] O. Glatter, O.Kratky. Small Angle X-ray Scattering, Academic Press. New York,1982
[7] J. W. Evancho, J.T.Staley, Metall.Trains [J].1974,5:43
[8] R.Delasi, P.N. Adler. Metall.Trans.,1977, 8A:1177-1183.
[9] P.N. Adler, R. Delasi. Metall. Trans ., 1977,8A:1185-1190.
[10] L.K.Berg, J.Gjonnes, V. Hansen et al. Acta mater,2001,49:3443-3451
[11] Deschamps, F.Livet, Y.Bréchet. Acta Mater,1999,47(1):281-292.